

Relaxation kinetics of stretched disclination lines in a nematic liquid crystalNatan Osterman,^{1,2,3,*} Juri Kotar,^{1,2} Eugene M. Terentjev,¹ and Pietro Cicuta^{1,2}¹*Cavendish Laboratory, University of Cambridge, Cambridge CB3 0HE, United Kingdom*²*Nanoscience Centre, University of Cambridge, Cambridge CB3 0FF, United Kingdom*³*Jozef Stefan Institute, Jamova 39, 1000 Ljubljana, Slovenia*

(Received 9 February 2010; published 3 June 2010)

The dynamics of disclination defect lines in a nematic liquid crystal are measured experimentally and considered theoretically. An optical trap is used to deform the line, enabling the previously unexplored regime of large deformation to be accessed. The relaxation follows a linear decay at large amplitude, crossing over into the well understood exponential decay at small amplitude. Both regimes can be described by simple theoretical arguments. The crossover point is well described by the theory, but the experiments show a faster than expected dynamics, indicating that the effective viscosity in the models is overestimated.

DOI: [10.1103/PhysRevE.81.061701](https://doi.org/10.1103/PhysRevE.81.061701)

PACS number(s): 42.70.Df, 61.30.Jf, 83.10.Mj

I. INTRODUCTION

In the same way that hard condensed matter crystals can be made more interesting and useful by doping to induce defects and irregularities, the presence of defects in liquid crystalline (LC) phases opens up a playground for soft matter physics, with the prospect of a better understanding of the material properties and ultimately the possibility of new applications. Topological defects can occur as metastable states during symmetry breaking phase transitions, or they can be induced under external fields or as equilibrium structures nucleated by impurities. Today there is a renewed interest in topological defects and especially their dynamics, motivated by their role in liquid crystal/colloidal particle composites. Colloidal inclusions alter the otherwise homogeneous director field and give rise to structural forces not observable in ordinary fluids [1–3]. The results of long range structural forces are fascinating self-ordered colloidal structures, such as chains [4], two-dimensional (2D) crystals [5], regular arrays of defects etc. (for a review see [3,6]).

The simplest LC phase is the uniaxial nematic; line defects are referred to as disclinations. Defects in LC phases can usually be directly observed in polarized optical microscopy. In general the study of the shape and dynamics of defects provides a powerful tool to probe the material properties: elastic constants and viscosities. In particular the dynamics of a disclination movement offers a route to understand the orientational friction and viscous coefficients in liquid crystals. The first attempt to study friction this way was by Imura and Okano [7], who obtained a closed expression for the friction force acting on a disclination line if it were to move with a constant velocity in the nematic matrix. This result was later improved in different ways (e.g., [8]) and has led to famous results on the dynamics of disclination coarsening (showing that the mesh size of a disclination network decreases as $l \sim t^{1/2}$) [9] or direct measurements of contracting disclination loops (the loop radius decreasing as $R \sim t^{1/2}$) [10].

A particularly useful tool to manipulate the colloids and defects in LC are laser tweezers. Contrary to what happens in

simple fluids, colloids can be trapped and manipulated even though the index of refraction of the particles is lower than both indices of refraction of the surrounding nematic matrix [11]. Two mechanisms are known to be responsible for such anomalous trapping: (a) surface-induced distortion of the birefringent media around the particle creates a high-index cloud around the colloid, and (b) laser induced distortion or (partial) melting of a nematic, which creates a “ghost colloid” at the focal spot. The focused laser beam can also move director structures and defects [12,13]. At low-laser power, the trapping is mediated by optical gradient forces exerted by a focused beam on the structures with spatially varying molecular orientations. When manipulation is done with high-intensity beams ($j > 4 \times 10^6$ W/m²) the tightly focused polarized laser beam locally reorients the director and causes an optical Freedericks transition. The elastic structural forces arise to minimize the distortions in the elastic LC medium.

In this paper, we present a simple experimental system which allows us to test basic theories of disclination energy and dissipative motion. We use a focused laser beam to stretch and otherwise deform defect lines, and we measure the kinetics of their motion in a planar cell of nematic liquid crystal. We test our system on a classical contracting-loop dynamics and then measure the friction of confined defect lines that relax to the equilibrium position.

II. THEORETICAL MODEL

The tension of a disclination line in bulk can be approximated by [14]:

$$T = \pi K s^2 \frac{L}{r_c} + \pi \sigma_c r_c^2, \quad (1)$$

where K is the average Frank elastic constant (in the qualitatively meaningful one-constant approximation [14]), s the strength of disclination and L is the effective size of the system (the linear dimension of the region of director deformations around the disclination line). Parameters r_c and σ_c represent the disclination core size and energy density, respectively.

When a disclination line moves through the director field, it experiences an effective dissipative friction with the force

*natan.osterman@jjs.si

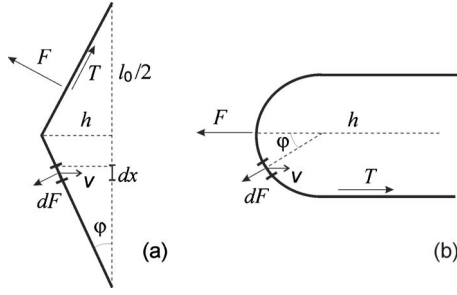


FIG. 1. Schematic view of the forces acting on a disclination in two deformation modes. T is the tension, F is the net friction force, h is the distance between tip and the equilibrium position, l_0 is the equilibrium length of the disclination. (a) Triangular mode and (b) Overstretched disclination model (v and dF are the local velocity and friction force acting on a short segment of disclination).

per unit length acting perpendicular to the line. In the same approximations as the basic expression for the disclination line tension [Eq. (1)] the friction coefficient is given by the Imura-Okano expression [7]:

$$R = \pi\gamma s^2 \ln \frac{L}{r_c}, \quad (2)$$

with γ being the rotational viscosity coefficient of the nematic. If a straight segment of a disclination line of length dl is moving through surrounding medium with velocity v and angle φ between v and the segment, then the frictional force dF acts perpendicular to the segment and is given by:

$$dF = Rv_{\perp} dl = Rv \cos \varphi dl. \quad (3)$$

If a middle point of an initially straight disclination of equilibrium length l_0 is pulled a distance h_0 away from the equilibrium position, the line shape becomes triangular (the defect line is straightened under tension between the tip of the disclination and pinning points), as sketched in Fig. 1(a). The relaxation of a stretched disclination back to its equilibrium position can be modeled as a motion of an overdamped (massless) string. Assuming that the triangular shape is preserved during the relaxation, the time dependence of the distance $h(t)$ between the tip of the disclination and its equilibrium position can be calculated analytically. The velocity $v(x)$ of a line segment is given by the linear proportionality, $v(x) = (dh/dt)(2x/l_0)$. The total friction F acts perpendicular to the disclination line and its magnitude for one half of the defect line is given by adding together all elements of dF for $dl = dx \cos \varphi$:

$$F = \int Rv_{\perp} dl = \int_0^{l_0/2} R \frac{dh}{dt} \frac{2x}{l_0} dx = \frac{Rl_0}{4} \frac{dh}{dt}. \quad (4)$$

During the movement of the disclination, the y components of the tension and the friction must have the same magnitude: $T \sin \varphi = F \cos \varphi$, or equivalently $Th = (l_0/2)F = (l_0^2/8)R(dh/dt)$. This relationship describes the simple exponential relaxation of $h(t)$ with the solution:

$$h(t) = h_0 e^{-t/\tau}, \quad (5)$$

with the characteristic relaxation rate $\tau^{-1} = 8T/l_0^2 R$.

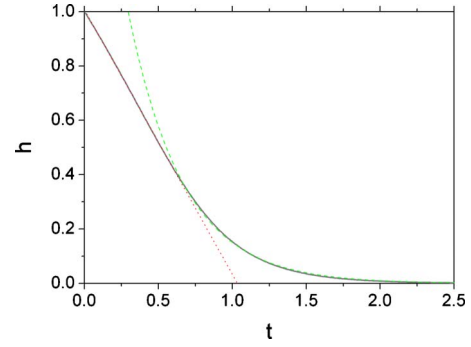


FIG. 2. (Color online) Numerical solution for the relaxation of parabolic shape. In nondimensional units, the equilibrium length of the disclination was taken as $l_0=2$, the initial displacement of the tip $h(0)=1$ and the ratio between tension and friction $T/R=1$. Two distinct phases of relaxation can be easily deduced. The data from $t=0$ to $t=0.6$ is fitted by the linear decay, while the final approach to equilibrium (data from $t=0.6$ to $t=2.5$) is fitted by the simple exponential.

The other limiting case is the relaxation of an overstretched disclination [sketched in Fig. 1(b) and shown in the top-most image of Fig. 5 below], where the length of the stretched defect line is significantly longer than the length of equilibrated disclination l_0 . In this case the size of the “hairpin” (the approximately semi-circular disclination region oriented at an angle to the direction of movement) remains constant during the main part of the relaxation. The total frictional force is produced by this hairpin region only and obtained by integrating the elements dF along the arc projected upon the axis:

$$F = \int Rv_{\perp}(l) \cos \varphi dl = \int_{-\pi/2}^{\pi/2} R \frac{dh}{dt} \cos^2 \varphi \frac{\xi}{2} d\varphi = \frac{\pi R \xi}{4} \frac{dh}{dt}, \quad (6)$$

where ξ is the width of the hairpin. By equating the total friction force and the tension acting on both ends of the hairpin segment, one obtains the differential equation describing its motion: $\frac{1}{4}\pi\xi R(dh/dt) = 2T$. The conclusion is that the retraction of the overstretched disclination, $h(t)$, proceeds linearly with time,

$$h(t) = h_0 - kt, \quad (7)$$

with the rate of retraction given by $k = 8T/\pi\xi R$. Note that in all cases the rate of relaxation is determined by the ratio of the disclination tension to the friction coefficient.

We have also modeled the disclination relaxation process by using the parabolic rather than triangular shape of the stretched line as an example of a more complex model that is closer to experimental observation. The assumption of the model is that the shape of the disclination remains parabolic during the whole relaxation to equilibrium, i.e., the shape at some given h can be described by $y(x, h) = h(4x^2/l_0^2 - 1)$. Such a problem is harder to solve analytically, but numerical solution reveals two different regimes of $h(t)$: the initial linear part of the relaxation, followed by an exponential decay. Figure 2 shows the time evolution of $h(t)$ for a disclination of

parabolic shape. The relaxation of $h(t)$ starts as a linear function which smoothly crosses over to an exponential decay at around $t=0.6$. The slope of linear decay k and characteristic relaxation time τ of the parabolic model have prefactors that are close to those obtained in the simple models described above. For example, the relaxation time in the parabolic model is $\tau=l_0^2R/12T$, which is 33% less than τ in the simple linear model. Considering that in practice the quantities T and R carry a large experimental uncertainty, and that our theoretical treatment is done in the realm of the one-elastic constant approximation, even the simple models seem an appropriate description of the relaxation.

III. EXPERIMENTAL METHODS

The negative photoresist SU-8 (Microchem Corp, MA, USA) was employed to create $15\ \mu\text{m}$ deep regions on cleaned standard glass microscope slides. The regions were then filled with nematic liquid crystal mixture E7 (Merck, Darmstadt, Germany) with average refractive index $n_{LC} \approx 1.6$, birefringence $\delta n \approx 0.2$, and rotational viscosity $\gamma_1 = 0.19\ \text{Pa}\cdot\text{s}$. The upper surface of LC was free (cells were not covered) and no special treatment for surface alignment was used. In these conditions, it is expected that the bottom surface of contact with SU8 will have planar director, while the top free surface will have a weak homeotropic anchoring.

To manipulate the LC defect we used a laser tweezers setup made of a CW laser (IPG Photonics, PYL-1-1064-LP, $\lambda=1064\ \text{nm}$, $P_{max}=1.1\ \text{W}$) focused through a water immersion objective (Zeiss, Achroplan IR 63x/0.90 W) in inverted microscope configuration. A pair of acousto-optic deflectors, driven by custom made electronics controlled by a personal computer, was used to move the optical trap and change its intensity. The sample was illuminated with a halogen lamp and observed in bright field with a CMOS camera (Allied Vision Technologies, Marlin F-131B) at a rate of 20 frames per second. Further details on the experimental setup are given in [15]. The positions of the defect lines were analyzed off-line with image analysis software (Able Image Analyzer, Mu Laboratories).

IV. RESULTS AND DISCUSSION

In our experiment, we used a high-intensity laser beam to manipulate the defect lines. Ramping up from zero intensity, first a laser spot becomes visible at certain threshold (ghost) but it cannot manipulate the director structures; at around $100\ \text{mW}$ of power focused to $1\ \mu\text{m}^2$ the optical trap can be used to push or pull a defect line. The optical force acting on the disclination is laser power dependent. If the optical trap is used to pull the mid point of a straight disclination into a triangular configuration, the maximum achievable opening angle θ_{max} of the triangle depends on the laser intensity. If the trap is pulled even further away, the defect line snaps and relaxes to equilibrium position. In Fig. 3, we show the dependence of the maximum angle of the defect line as a function of laser beam intensity. When the laser power in the sample is below $100\ \text{mW}$ it cannot be used to pull the disclination (i.e., the angle is 180 degrees). With increasing

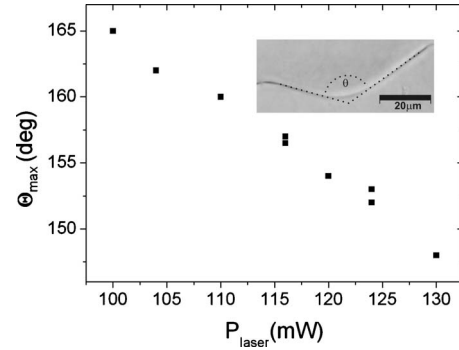


FIG. 3. There is a linear dependence between the maximum amplitude of deformation and the applied laser power. The data represent the maximum angle θ_{max} of the tip of disclination at each laser trap power (measured at sample).

power the maximum achievable angle decreases and at around $140\ \text{mW}$ (in the case of the observed disclination) the force is high enough to completely pull the tip of disclination and drag it to an arbitrary position.

We believe that the main effect of the laser on the defect structure is due to heating. The interaction force between laser trap and the disclination is created by producing a radial distribution of the nematic order parameter around a locally isotropic region created by IR laser heating, similar to the report in [16] and to the well-known effect of colloidal assembly on disclination lines which reduces the local core energy.

First we tested our experimental setup on classical contracting-loop dynamics. The laser beam was focused to a dust particle with high IR absorption. The local heating of the particle induced nematic to isotropic transition (limited to a circular region with a size of a couple of tens of micrometers), and produced some long disclination lines around the spot. When the laser beam was moved away from the absorbing particle, the isotropic region of LC was quenched back to nematic phase in $\sim 1\ \text{s}$. If any defect loop remained after the quenching, we pulled it away from the dirt using the laser tweezers, and started to observe its contraction.

In Fig. 4, we show the time evolution of the ellipsoidal contracting loop. The time dependence of ellipsoidal major a_1 and minor axis a_2 was fitted with the power-law function $a_i(t)=A_{0i}(t_0-t)^{\beta_i}$. We obtained $\beta_1=0.516 \pm 0.005$, and $\beta_2=0.490 \pm 0.006$ which is in excellent agreement with theoretical predictions [10].

The main focus of this paper is the relaxation of straight disclination lines with their ends pinned either to SU-8 film or to the glass surface. By using the focused laser beam, the disclinations were pulled similarly to an elastic string. When the optical trap was switched off, the disclinations started to relax back to the equilibrium position. From the video we measured the distance $h(t)$ between the “tip” of the defect line and the final position of the relaxed line as a function of time. By observing the relaxation of different disclination lines (different lengths, thicknesses of the liquid crystal layer, pinning configurations) we found out that relaxations consist of two stages. When the disclination is relaxed from a strongly stretched state, the shape of the disclination hairpin remains unchanged, and only the lines between the hairpin

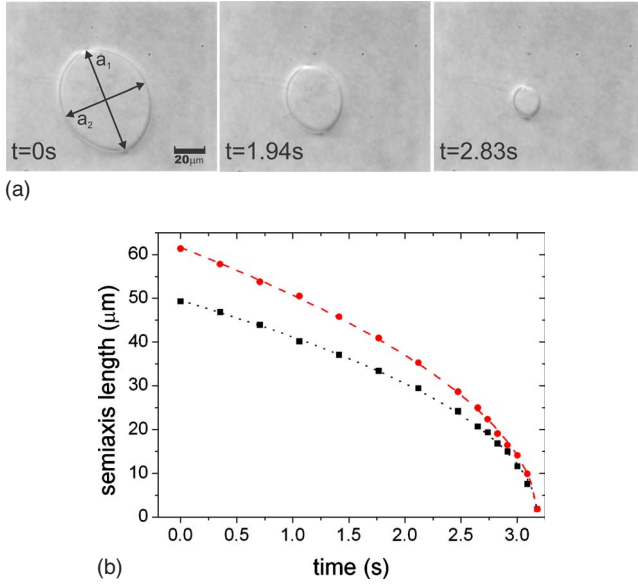


FIG. 4. (Color online) Contraction of ellipsoidal disclination follows theoretical expectation. (a) Image sequence of contracting loop. (b) The time evolution of the distance of long (circles) and short axes (squares) of ellipses. The data is fitted with power law functions giving exponents $\beta_1=0.516 \pm 0.005$ (red line) and $\beta_2=0.490 \pm 0.006$ (black line).

and the pinning points shorten (Fig. 1 right). The viscous drag is constant in this process, therefore the disclination tip approaches the equilibrium position with constant speed as calculated in Eq. (7). As the disclination comes closer to the equilibrium position, the shape of the disclination “cap” is changing, and this modifies both the effective viscous drag and the angle at which tension is pulling the disclination tip. The $h(t)$ shows an exponential decay in this stage [Eq. (5)]. If the disclination is relaxed from an only slightly stretched state, then there is only one stage, that of exponential relaxation.

A series of micrographs of two typical relaxations of defect lines are presented in Figs. 5 and 6. The relaxation of an overstretched disclination with equilibrium length of $l_0=65 \mu\text{m}$, and the time dependence of the distance $h(t)$ between relaxation tip and equilibrated position of the line, are shown in Fig. 5. Both the initial linear and subsequent exponential stages of relaxation can be clearly seen in the chart.

The set of data points at small times in Fig. 5 was fitted with a linear function with slope $k=-10.4 \pm 0.2 \mu\text{m/s}$, the set at large times was fitted with an exponential decay with characteristic decay time $\tau=0.8 \pm 0.1 \text{ s}$. The ratio $\delta=T/R$ between tension and friction coefficients is related to both fitted values as $\delta=\pi l_0 k/8=2.6 \times 10^{-10} \text{ m}^2/\text{s}$ and $\delta=l_0^2/8\tau=6.5 \times 10^{-10} \text{ m}^2/\text{s}$.

A series of relaxation images of a just slightly stretched disclination with equilibrium length $l_0=107 \mu\text{m}$ in another cell is presented in Fig. 6. In this case the evolution of $h(t)$ is a pure exponential decay, with $\tau=10.0 \pm 0.2 \text{ s}$. The ratio between tension and friction coefficient in this case is $\delta=1.43 \times 10^{-10} \text{ m}^2/\text{s}$.

The tension and friction coefficient can be estimated directly from Eqs. (1) and (2). Assuming that the topological

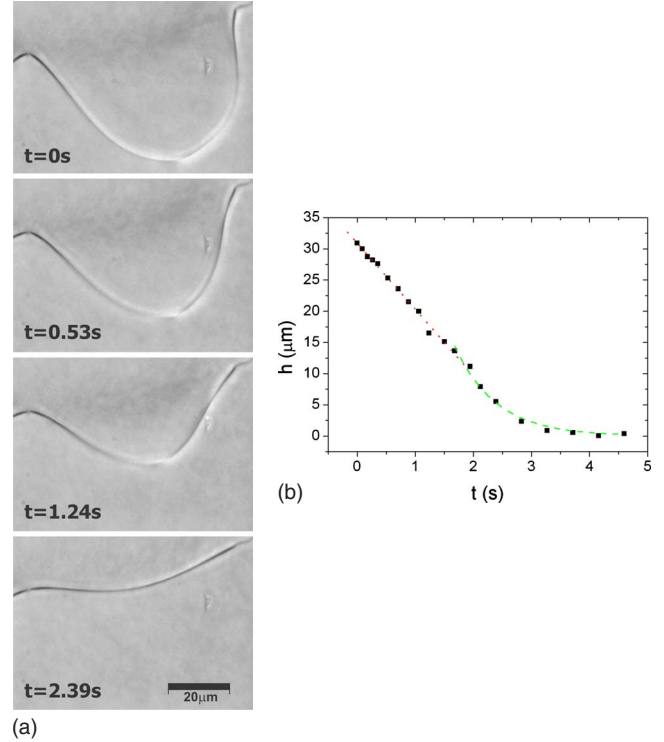


FIG. 5. (Color online) Relaxation of overstretched disclination shows two regimes. (a) Brightfield images of disclination at different times after relaxation. The laser spot is clearly seen below the tip of the disclination in the top image. This disclination has $l_0=65 \mu\text{m}$. (b) Time evolution of distance $h(t)$ between ‘tip’ of disclination and its equilibrium position. The dotted line is a fit of the experimental data (points 1–13) with a linear function of slope $k=-10.6 \pm 0.3 \mu\text{m/s}$, the dashed line is an exponential fit (data points 13–19) with decay constant $\tau=0.72 \pm 0.06 \text{ s}$.

strength of observed disclinations is $s=1/2$ [20], the size of system is around $L=10 \mu\text{m}$, the average elastic constant and rotational viscosity of E7 at room temperature are $K=13.5 \text{ pN}$ and $\gamma=257 \text{ mPa s}$ [17], respectively; the radius of the disclination core $r_c=5 \text{ nm}$ and $\sigma_c \approx K/r_c^2$, which gives the total tension of disclination $T=123 \text{ pN}$ and the friction coefficient $R=1.5 \text{ Pa s}$. The estimated ratio between tension and friction is therefore $\delta=0.8 \times 10^{-10} \text{ m}^2/\text{s}$, in reasonable agreement with the experiments.

In Figs. 5 and 6, the pinning points are on the bottom surface. We observe that the line can be moved freely and repeatedly with the optical trap and that the relaxation is smooth. This convinces us that the disclination line is not itself pinned to the bottom, since one would expect in that case a complex dynamics controlled by depinning events. One aspect to consider is the position of the disclination line relative to the bottom surface. If the disclination line is separate, but close (of the order of the core size, i.e., 5 nm) to the bottom, then the drag of the core across the surface roughness could contribute to the dynamics. The optical resolution in the z direction (which would appear as defocusing) is of the order of one micron, and therefore not precise enough to establish if this condition is held. In Fig. 5, the contrast on the disclination is different from that near the pinning points, and one possible origin of this could be that the disclination

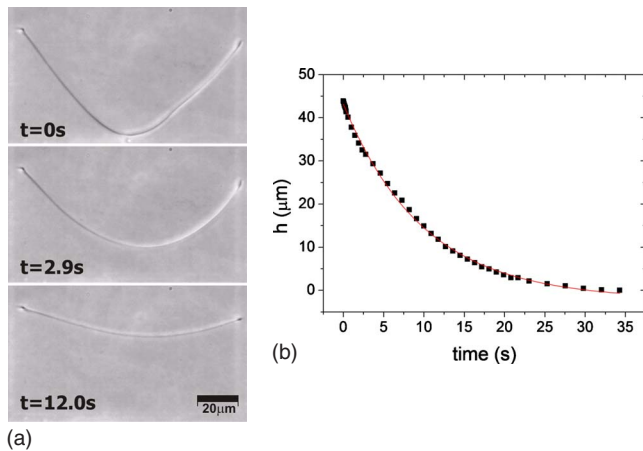


FIG. 6. (Color online) Simple relaxation of disclination. (a) Brightfield images of disclination at different times after relaxation. This disclination has $l_0=107 \mu\text{m}$. The laser spot is clearly seen below the tip of the disclination in the top image. (b) Time evolution of the distance $h(t)$ between the tip of the disclination and its equilibrium position. The line is an exponential fit of the data, with decay constant $\tau=10.0 \pm 0.2 \text{ s}$.

tilts upwards, away from the bottom surface by a fraction of a micrometer. Assuming that the disclination and the boundary are farther than the core size, and knowing the theoretical tension and friction of the disclination, the characteristic decay time τ of Eq. (5) can be predicted. For the shorter disclination in Fig. 5, this is $\tau=l_0^2 R/8T=7 \text{ s}$, and for the disclination in Fig. 6 $\tau=19 \text{ s}$. Measured values of characteristic decay times are somewhat shorter than predictions by our simple models. This discrepancy confirms a finding previously reported in [18]. In that work the equilibrium fluctuation modes of defect lines were analyzed, and it was possible to obtain the tension and effective viscosity. While the tension was found to compare well with theory, the viscous

coefficient found in experiment was less than half what is expected from simple theory, which is what we report in the current work. The origin of this discrepancy lies in the neglecting the coupling of flow and reorientation of the nematic order (backflow), in obtaining Eq. (2). This makes Eq. (2) only applicable in the limit of extremely slow movements of the disclination line. The experiments in this work (and [18]) indicate that this leads to a significant discrepancy in the time scale of relaxation. Modeling backflow requires numerical solution of the equations of nematohydrodynamics, and is beyond the scope of this paper. A calculation for the case of the motion of defects of strength $\pm 1/2$ was done in [19] and showed that the inclusion of backflow led to a doubling of the relaxation speed.

V. CONCLUSIONS

In this paper, we have considered experimentally and theoretically the relaxation of stretched disclination lines in nematic liquid crystals. Using optical manipulation and brightfield microscopy we have induced disclinations and observed two different modes of relaxation depending on the amplitude of deformation. The relaxations decayed either linearly or exponentially in time, a behavior that we explained qualitatively from simple theory considerations. The theory arguments used here neglect backflow and make simplifying assumptions on the elasticity of the nematic phase (one constant approximation). Experimentally the disclination strength and the distance between the disclination lines and the solid boundaries are not controlled. Despite these limitations, there is reasonable quantitative agreement between the simple predictions and experiments, with the observed relaxation times being shorter than expected.

ACKNOWLEDGMENT

We wish to thank Igor Poberaj for helpful discussions.

-
- [1] S. Ramaswamy, R. Nityananda, V. A. Raghunathan, and J. Prost, *Mol. Cryst. Liq. Cryst.* **288**, 175 (1996).
 [2] R. W. Ruhwandl and E. M. Terentjev, *Phys. Rev. E* **55**, 2958 (1997).
 [3] H. Stark, *Phys. Rep.* **351**, 387 (2001).
 [4] P. Poulin, H. Stark, T. C. Lubensky, and D. A. Weitz, *Science* **275**, 1770 (1997).
 [5] I. Muševič, M. Škarabot, U. Tkalec, M. Ravnik, and S. Žumer, *Science* **313**, 954 (2006).
 [6] P. M. Chaikin and T. C. Lubensky, *Principles of Condensed Matter Physics* (Cambridge University Press, Cambridge, U.K., 2000).
 [7] H. Imura and K. Okano, *Phys. Lett. A* **42**, 403 (1973).
 [8] G. Ryskin and M. Kremenetsky, *Phys. Rev. Lett.* **67**, 1574 (1991).
 [9] T. Nagaya, H. Hotta, and H. O. Y. Ishibashi, *J. Phys. Soc. Jpn.* **61**, 3511 (1992).
 [10] I. Chuang, N. Turok, and B. Yurke, *Phys. Rev. Lett.* **66**, 2472 (1991).
 [11] I. Muševič, M. Škarabot, D. Babič, N. Osterman, I. Poberaj, V. Nazarenko, and A. Nych, *Phys. Rev. Lett.* **93**, 187801 (2004).
 [12] I. I. Smalyukh, A. N. Kuzmin, A. V. Kachynski, P. N. Prasad, and O. D. Lavrentovich, *Appl. Phys. Lett.* **86**, 021913 (2005).
 [13] I. I. Smalyukh, D. S. Kaputa, A. V. Kachynski, A. N. Kuzmin, and P. N. Prasad, *Opt. Express* **15**, 4359 (2007).
 [14] P. G. de Gennes and J. Prost, *The Physics of Liquid Crystals*, 2nd ed. (Oxford University Press, Oxford, U.K., 1993).
 [15] M. Leoni, J. Kotar, B. Bassetti, P. Cicuta, and M. Cosentino Lagomarsino, *Soft Matter* **5**, 472 (2009).
 [16] S. A. Tatarkova, D. R. Burnham, A. K. Kirby, G. D. Love, and E. M. Terentjev, *Phys. Rev. Lett.* **98**, 157801 (2007).
 [17] H. Wang, T. X. Wu, S. Gauza, J. R. Wu, and S.-T. Wu, *Liq. Cryst.* **33**, 91 (2006).

- [18] A. Mertelj and M. Čopič, *Phys. Rev. E* **69**, 021711 (2004).
- [19] G. Tóth, C. Denniston, and J. M. Yeomans, *Phys. Rev. Lett.* **88**, 105504 (2002).
- [20] Assuming a disclination strength $s=1/2$ is plausible because it is the only strictly topologically stable type of disclination in a nematic. It is a possibility that the disclinations could be of

strength $s=1$ (but certainly not higher than that). In considering δ , the strength enters into both the energy and the friction contributions, and so the only place where the difference might be noticed is in the disclination-core term in Eq. (1). This modification has a minor effect on the estimates presented here.